ELECTROMAGNETIC HYDRODYNAMIC FLOW AND HEAT TRANSFER OF A CASSON NANOFLUID Fe_3O_4-BLOOD IN A POROUS MEDIUM

by

Jelena D. PETROVIĆ[a*], Milica D. NIKODIJEVIĆ DJORDJEVIĆ[b], and Miloš M. KOCIĆ[a]

[a] Faculty of Mechanical Engineering, Niš, Serbia
[b] Faculty of Occupational Safety, Niš, Serbia

Original scientific paper
https://doi.org/10.2298/TSCI230516169P

This paper discusses the fully developed electromagnetic hydrodynamic flow and heat transfer of a Casson nanofluid Fe_3O_4-blood in a porous medium. The flow takes place in a horizontal channel with walls at different temperatures. The channel is influenced by an externally applied magnetic field that is perpendicular to the walls of the channel and an externally applied electric field that is perpendicular to the longitudinal vertical plane of the channel. Both of these fields are homogeneous. The induced magnetic field is considered weak and can be neglected. The described problem is represented by differential equations which are analytically solved after the transformation into a dimensionless form. The obtained velocity and temperature distributions of the Casson fluid Fe_3O_4-blood are graphically represented and the influences of the Hartmann number, the Brinkman number, the power factor, the porosity factor, and the volume fraction of nanoparticles are examined. The Nusselt number and dimensionless friction voltages are given in a table.

Key words: *nanofluid, blood, porous medium, electromagnetic hydrodynamic, iron oxide*

Introduction

Convective heat transfer is ubiquitous in nature and in practice *e.g.*, in thermal insulation, heat exchangers, drying technology, petroleum industry, geothermal systems, energy storage, solar absorption, cooling of electronic devices, catalytic reactors, *etc.* One of the current techniques to improve heat transfer is the use of porous media and one of the latest solutions is the use of nanofluids, as proposed by Choi [1] in 1995. Over the last two decades researchers have focused heavily on the simultaneous use of a porous medium, nanofluids and a magnetic field owing to their potential scientific, technological, and industrial application. This led to considerable advancements regarding their application in biomedicine specifically in the production of replacement tissue, delivery of pharmaceuticals, advanced medical imaging, cancer treatment, treatment of cardiovascular diseases, cryopreservation and many more.

Umavathi and Sheremet [2] investigated the influence of magnetic and electric field on mixed convection flow through a vertical channel using Robin boundary conditions with a heat source/sink. Raju [3] studied the influence of the Hall current and the Coriolis force on

* Corresponding author, e-mail: jelena.nikodijevic.petrovic@masfak.ni.ac.rs

the flow and heat transfer of two immiscible fluids in a channel between two vertical plates. The channel was influenced by an electric and a magnetic field at constant plate temperatures. Raju [3] also suggested some practical applications for this model. Lima *et al.* [4] examined the flow and heat transfer of two immiscible fluids in an inclined channel with the presence of an electric field, an inclined magnetic field and an induced magnetic field with heat generation/absorption. The channel walls were moving and at constant but different temperatures. The authors considered viscous and Joule heating.

Petrović *et al.* [5] considered the flow and heat transfer of two immiscible fluids in a horizontal channel. The fluids flowed through parts of the channel with different porosity. The channel was influenced by an electric field and an inclined magnetic field and the channel walls were at constant but different temperatures. Krishna *et al.* [6] investigated the influence of thermal radiation and buoyancy force on entropy generation in the MHD flow of a Jeffrey fluid through a vertical microchannel filled with a porous medium. Kasaein *et al.* [7] provided a detailed review of the simultaneous use of porous media and nanofluids to improve heat transfer.

Sharma and Manjeet [8] studied nanofluid flow and heat convection in a channel filled with a porous medium and influenced by a magnetic field perpendicular to the channel walls. The top channel wall was porous with a variable temperature while the bottom wall was non-permeable at a constant temperature. Khanafer and Vafai [9] provided a detailed review of the application of nanofluids in porous media emphasizing natural and mixed convection and the MHD effect in a porous medium. They also proposed ideas for further research. Sheremet [10] gave a brief analysis of nanofluid application. Raveendra *et al.* [11] investigated the MHD flow and heat transfer of a Casson fluid in a vertical channel with stretching porous walls. They considered the heat source/sink, radiative heat and concentration.

Omokhuale and Jabaka [12] studied the effects of heat generation and chemical reaction on MHD flow and heat transfer of a Casson fluid over an infinite vertical plate immersed in a saturated porous medium. To solve the relevant equations they used the explicit finite difference method. Gireesha and Sindhu [13] investigated the combined influence of Joule heating, viscous dissipation, the Hall effect, and thermal radiation on entropy generation rate during the MHD Casson fluid flow through a vertical micro-channel with porous walls. To solve the relevant equations they used the Runge-Kutta-Fehlberg 45 method and MAPLE software. Eldabe *et al.* [14] studied the flow and heat transfer of a Casson fluid in an electromagnetic hydrodynamic (EMHD) boundary-layer over a horizontally-shrinking plate in a porous medium with viscous dissipation, Joule heating, heat generation, thermal diffusion and chemical reaction.

Khaled and Vafai [15] explored flow and heat transfer in biological tissues. They analyzed mass diffusion in tissue regeneration and in brain tissues, convection flow in biological tissues using different porous media models, bioheat equation and transport through porous media and bioconvection and the application of magnetic resonance in porous media. Srinivas *et al.* [16] investigated the flow and heat transfer of a gold-blood nanofluid in a horizontal porous channel with moving/stationary porous walls and under the influence of thermal radiation. The blood was considered a Newtonian fluid. The authors determined the analytical solutions using the homotopy analysis method. Noreen *et al.* [17] studied the influence of copper nanoparticles on peristaltic blood and heat transport in a vertical channel. The blood was modeled as a Boger pseudoplastic fluid.

Akhtar *et al.* [18] investigated the electrokinetic blood flow and heat transfer through an artery with multiple stenoses. The blood was modeled as a Casson fluid. Srinivas

et al. [19] studied the influence of radiative heat transfer on entropy generation during the flow of two immiscible non-Newtonian fluids between two horizontal plates which were at constant but different temperatures. They showed that heat generation decreases with thermal radiation and increases with viscous dissipation. Petrović *et al.* [20] investigated the EMHD nanofluid flow and heat transfer in a horizontal channel filled with a porous medium. The channel walls were horizontal plates at constant but different temperatures. The problem was analyzed by means of inductionless approximation.

Chinyoka and Makinde [21] numerically investigated the MHD flow and heat transfer in the blood vessel taking thermal radiation into account. Das *et al.* [22] theoretically investigated the MHD peristaltic flow and heat transfer of Casson hydride nanofluid Ag-Al_2O_3-blood through an endoscope taking into account Hall and ion currents, viscous and ion dissipation. Khan *et al.* [23] investigate the MHD flow and heat transfer of Casson nanofluid Au-blood in a rotating porous medium taking into account thermal radiation. Numerical investigation of MHD flow and heat transfer of blood in a stenosed curved artery was done by Sharma *et al.* [24]. The EMHD flow and heat transfer of hybrid nanofluid Al_2O_3-Cu-water on a stretching plate considering second order slip and heat source were investigated by Jawad *et al.* [25].

Khan *et al.* [26] investigated the flow and heat transfer of nanofluids in the boundary-layer in a porous medium on a horizontal stretching plate. Rehman *et al.* [27] analytically investigated the flow and heat transfer of nanofluids taking into account viscous dissipation and convective boundary conditions. The MHD flow and heat transfer of Casson nanofluids on a stretching surface were investigated by Rehman *et al.* [28]. Mixed convective flow of hybrid nanofluid CuO-Cu-blood with gyrotactic microorganisms over a horizontal porous stretching plate was analyzed by Alharbi *et al.* [29].

After an extensive literature review the authors of the present paper think that EMHD nanofluid flow and heat transfer in a porous medium has not been sufficiently explored especially when blood is used as the base fluid. Therefore the aim of this paper is to investigate the steady, complete, developed, and laminar EMHD nanofluid flow and heat transfer in a horizontal channel. The channel walls are horizontal plates at constant but different temperatures. The channel is filled with a porous medium which is considered as a Darcy model. Blood is used as the base fluid and considered as a Casson model while the nanoparticles are iron oxide (Fe_3O_4). The applied external magnetic field is homogeneous and perpendicular in relation to the plates while the electric field is homogeneous and perpendicular in relation to the longitudinal vertical plane of the channel. Analytical solutions of the analyzed problem are determined for velocity distributions and temperatures of the nanofluid, skin frictions, and Nuselt numbers. The solutions are represented graphically and tabulary. The influence of the introduced physical parameters is then discussed.

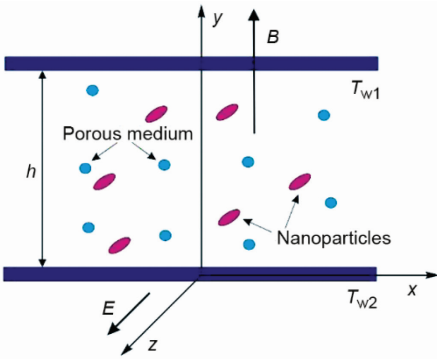

Figure 1. Physical configuration

Formulation of the problem

The nanofluid with blood as its base flows through a horizontal channel between parallel plates. The primary flow proceeds along the x-axis of the adopted co-ordinate system, fig. 1. The plates are at constant but different temperatures T_{w1} and T_{w2}. The

external magnetic field with induction, B, is homogeneous and perpendicular to the plates while the external electric field, E, is homogeneous and follows the direction of the z-axis.

The impulse and energy equations of the described problem for the adopted co-ordinate system have the following forms:

$$-\frac{\partial p}{\partial x}+\left(1+\frac{1}{\gamma}\right)\mu_{\mathrm{nf}}\frac{\mathrm{d}^2u}{\mathrm{d}y^2}-\left(1+\frac{1}{\gamma}\right)\frac{\mu_{\mathrm{nf}}}{K_0}u-B\sigma_{\mathrm{nf}}(E+Bu)=0 \tag{1}$$

$$k_{\mathrm{nf}}\frac{\mathrm{d}^2T}{\mathrm{d}y^2}+\left(1+\frac{1}{\gamma}\right)\mu_{\mathrm{nf}}\left(\frac{\mathrm{d}u}{\mathrm{d}y}\right)^2+\left(1+\frac{1}{\gamma}\right)\frac{\mu_{\mathrm{nf}}}{K_0}u^2+\sigma_{\mathrm{nf}}(E+Bu)^2=0 \tag{2}$$

The corresponding boundary conditions for velocity and temperature are:

$$u(0)=0,\quad u(h)=0,\quad T(0)=T_{\mathrm{w}_2},\quad T(h)=T_{\mathrm{w}_1} \tag{3}$$

Equations (1) and (2) and boundary conditions (3) contain the following symbols: x and y are the longitudinal and transversal Cartesian co-ordinate, u is the fluid velocity, μ_{nf}, σ_{nf}, and k_{nf} – the dynamic viscosity, electrical conductivity, and thermal conductivity of nanofluid, respectively, K_0 – the permeability of the medium in the channel, T – the fluid temperature, γ – the Casson parameter, and h – the channel height.

The physical properties of the nanofluid are:

$$\mu_{\mathrm{nf}}=\mu_{\mathrm{f}}\varphi_1^{-1},\quad k_{\mathrm{nf}}=k_{\mathrm{f}}\varphi_2,\quad \sigma_{\mathrm{nf}}=\sigma_{\mathrm{f}}\varphi_3 \tag{4}$$

with the symbols:

$$\varphi_1=(1-\phi)^{2.5},\quad \varphi_2=F(k),\quad \varphi_3=F(\sigma),\quad k=\frac{k_s}{k_{\mathrm{f}}},\quad \sigma=\frac{\sigma_s}{\sigma_{\mathrm{f}}},\quad F(\xi)=\frac{2(1-\phi)+(1+2\phi)\xi}{2+\phi+(1-\phi)\xi} \tag{5}$$

where μ_{f}, k_{f}, and σ_{f} are the viscosity, thermal conductivity, and electrical conductivity of the base fluid, respectively, k_s and σ_s – the thermal conductivity and electrical conductivity of the nanoparticles, respectively, and φ – volume fraction of the nanoparticles.

Solution

Using the physical properties of nanofluids (4) and by introducing the dimensionless variables:

$$y^*=\frac{y}{h},\quad u^*=\frac{u}{U},\quad \Theta=\frac{T-T_{\mathrm{w}_2}}{T_{\mathrm{w}_1}-T_{\mathrm{w}_2}} \tag{6}$$

where U is the reference velocity whose selection allows for a certain degree of arbitrariness, eqs. (1) and (2) are transformed into the following dimensionless equations:

$$\frac{\mathrm{d}^2u}{\mathrm{d}y^2}-\omega^2u=A \tag{7}$$

$$\frac{\mathrm{d}^2\Theta}{\mathrm{d}y^2}+\mathrm{Br}\left[b\left(\frac{\mathrm{d}u}{\mathrm{d}y}\right)^2+b\Lambda u^2+c\mathrm{Ha}^2(K+u)^2\right]=0 \tag{8}$$

In the last two equations and in the remainder of the paper below the symbol * has been excluded for the sake of simplicity but the dimensionless quantities still apply and the following symbols are used:

$$a_1 = \frac{\gamma}{1+\gamma}, \quad a = a_1\varphi_1\varphi_3, \quad a_2 = a_1\varphi_1 P_1, \quad P = -\frac{\partial p}{\partial x} = \text{const.}, \quad \Lambda = \frac{h^2}{K_0}, \quad K = \frac{E}{BU}$$

$$\text{Ha} = Bh\sqrt{\frac{\sigma_\text{f}}{\mu_\text{f}}}, \quad \omega^2 = \Lambda + a\text{Ha}^2, \quad A = aK\text{Ha}^2 - a_2, \quad b = \frac{1}{a_1\varphi_1\varphi_2}, \quad \text{Pr} = \frac{\mu_\text{f} c_{p,\text{f}}}{k_\text{f}} \tag{9}$$

$$\text{Ec} = \frac{U^2}{c_{p,\text{f}}(T_{\text{w}1} - T_{\text{w}2})}, \quad c = \frac{\varphi_3}{\varphi_2}, \quad \text{Br} = \text{Pr}\,\text{Ec}, \quad P_1 = P\frac{h^2}{\mu_\text{f} U}$$

where Λ is the porosity factor, K – the external power factor, Ha – the Hartmann number, Pr – the Prandtl number, Ec – the Eckert number, and Br – the Brinkman number.

Boundary conditions (3) are transformed into:

$$u(0) = 0, \quad u(1) = 0, \quad \Theta(0) = 0, \quad \Theta(1) = 1 \tag{10}$$

Solution of eq. (7) was got by the usual procedure for solving ordinary linear differential equations with constant coefficients and yields the following expression for nanofluid velocity distribution in the channel:

$$u(y) = C_1 \exp(\omega y) + C_2 \exp(-\omega y) + D \tag{11}$$

where quantity D and integration constants C_1 and C_2 are:

$$D = -\frac{A}{\omega^2}, \quad C_1 = \frac{D}{D_1}[\exp(-\omega) - 1], \quad C_2 = \frac{D}{D_1}[1 - \exp(\omega)], \quad D_1 = \exp(\omega) - \exp(\omega_1) \tag{12}$$

Input of velocity distribution (11) into equation (8) and its solution yield the following expression for the distribution of dimensionless nanofluid temperature in the channel:

$$\Theta(y) = -\text{Br}[R_4 \exp(2\omega y) + R_5 \exp(-2\omega y) + R_7 \exp(\omega y) + \\ + R_8 \exp(-\omega y) + R_2 y^2 + C_3 y + C_4] \tag{13}$$

where the following symbols were used for the sake of simplicity:

$$R_1 = b\Lambda + c\text{Ha}^2, \quad R_2 = \frac{1}{2}[R_1 D^2 + cK\text{Ha}^2(2D + K)], \quad R_3 = \frac{1}{4\omega^2}(b\omega^2 + R_1)$$
$$R_4 = R_3 C_1^2, \quad R_5 = R_3 C_2^2, \quad R_6 = \frac{2}{\omega^2}(DR_1 + cK\text{Ha}^2), \quad R_7 = R_6 C_1, \quad R_8 = R_6 C_2 \tag{14}$$

while integration constants C_3 and C_4 are given as the following expressions:

$$C_3 = -\frac{1}{\text{Br}} + R_4[1 - \exp(2\omega)] + R_5[1 - \exp(-2\omega)] + R_7[1 - \exp(\omega)] + R_8[1 - \exp(-\omega)] - R_2$$
$$C_4 = -(R_4 + R_5 + R_7 + R_8) \tag{15}$$

Dimensionless tangential stresses on the bottom and top channel walls are:

$$\tau_1 = \left(1 + \frac{1}{\gamma}\right)\frac{\mu_\text{nf}}{\mu_\text{f}}\left.\frac{\text{d}u}{\text{d}y}\right|_{y=0} = \frac{\omega}{a_1\varphi_1}(C_1 - C_2) \tag{16}$$

$$\tau_2 = \left(1+\frac{1}{\gamma}\right)\frac{\mu_{\mathrm{nf}}}{\mu_{\mathrm{f}}}\frac{\mathrm{d}u}{\mathrm{d}y}\bigg|_{y=1} = \frac{\omega}{a_1\varphi_1}[C_1\exp(\omega) - C_2\exp(-\omega)] \tag{17}$$

respectively, while the local Nusselt numbers on the bottom and top channel walls are:

$$\mathrm{Nu}_1 = -\frac{k_{\mathrm{nf}}}{k_{\mathrm{f}}}\frac{\mathrm{d}\theta}{\mathrm{d}y}\bigg|_{y=0} = \varphi_2\mathrm{Br}[2\omega(R_4 - R_5) + \omega(R_7 - R_8) + C_3] \tag{18}$$

$$\mathrm{Nu}_2 = -\frac{k_{\mathrm{nf}}}{k_{\mathrm{f}}}\frac{\mathrm{d}\theta}{\mathrm{d}y}\bigg|_{y=1} = \varphi_2\mathrm{Br}\{2\omega[R_4\exp(2\omega) - R_5\exp(-2\omega)] + \\ +\omega[R_7\exp(\omega) - R_8\exp(-\omega)] + 2R_2 + C_3\} \tag{19}$$

Result analysis

This section presents the results for the case when $P_1 = 1$ which is a frequent occurrence in the literature. This case corresponds with the selection of reference velocity, U, in the form $U = Ph^2/\mu_{\mathrm{f}}$. The physical properties of blood (base fluid) and the iron(II) iron(III) oxide (Fe_3O_4) nanoparticles are shown in tab. 1.

Table 1. Physical properties

Substance	ρ [kgm^{-3}]	k [WK^{-1}m^{-1}]	c_p [Jkg^{-1}K^{-1}]	σ [sm^{-1}]	μ [Pa·s]
Blood	1,053	0.492	3,594	0.8	$3.5\cdot10^{-3}$
Fe_3O_4	5,180	9.7	670	25,000	–

Figure 2 shows the dimensionless velocity profiles of the nanofluid in the channel for different values of the Hartmann number and for the external power factor of $K = \pm1$ while fig. 3 shows the dimensionless temperature profiles for different Hartmann values and for K = –1. As the Hartmann values change so does the magnetic field induction. Increase in the Hartmann values also increases the intensity of the Lorentz force which in turn increases the fluid velocity in the channel and tangential stresses on channel walls, as shown in fig. 2.

The results shown in tab. 2 indicate that the stresses have the same value on both channel walls which is due to velocity distribution symmetry. As the Hartmann number increases so does Joule heating causing the temperature increase in the channel, as shown in fig. 3.

The exchanged amounts of heat between the fluid and the channel walls are increased at higher Hartmann values. At the analyzed Hartmann values the bottom wall is heated whereas the top wall is heated at Ha = 4 and Ha = 6 at cooled at Ha = 2. These conclusions are verified by the results given in tab. 2.

When factor K changes, all the other factors remaining constant, the intensity and direction of the external electric field also change. Figure 4 shows that higher values of $|K|$ correspond to higher velocities and higher tangential stresses on channel walls. Similarly, fig. 5 shows that higher values of $|K|$ correspond to higher nanofluid temperatures in the channel which is due to higher Joule heating as a result of increase in $|K|$. For $K = 0$ (short-circuit mode) temperature profile is linear. As $|K|$ increases the exchanged amount of heat between the nanofluid and the channel walls increases on the bottom wall and decreases on the top wall. For $K = -0.5$ and $K = 0$ the bottom wall is heated whereas the top wall is cooled which can be concluded form the analysis of the results given in tab. 2.

Table 2. Nusselt number and wall friction values for parameter values Ha = 2, $K = -1$, $\phi = 0.02$, Br = 0.5, $\Lambda = 5$, $\gamma = 0.3$, and other parameter variations

	τ_1	τ_2	Nu_1	Nu_2
Ha				
2	1.8068	–1.8068	–2.06489	–0.04035
4	5.483512	–5.48351	–4.59307	2.487832
6	10.17818	–10.1782	–7.72948	5.624246
Λ				
5	1.8068	–1.8068	–2.06489	–0.04035
10	1.47417	–1.47417	–2.07644	–0.02879
15	1.266371	–1.26637	–2.08354	–0.0217
50	0.733756	–0.73376	–2.10064	–0.0046
500	0.23434	–0.23434	–2.11214	0.006904
ϕ				
0	1.723128	–1.72313	–1.9546	–0.0454
0.01	1.764526	–1.76453	–2.00921	–0.04295
0.02	1.8068	–1.8068	–2.06489	–0.04035
K				
–1	1.8068	–1.8068	–2.06489	–0.04035
–0.5	1.075644	–1.07564	–1.30784	–0.79739
0	0.344489	–0.34449	–1.05549	–1.04974
γ				
0.1	1.857587	–1.85759	–2.09385	–0.01138
0.3	1.8068	–1.8068	–2.06489	–0.04035
0.6	1.757993	–1.75799	–2.03707	–0.06817
Br				
0.5	–	–	–2.06489	–0.04035
1	–	–	–3.07715	0.971918
2	–	–	–5.10169	2.996455

As the porosity factor changes so does the permeability of the porous medium. Increase in the porosity factor decreases the permeability of the porous medium and increases the intensity of the resistance force within it. Additionally increase in the porosity factor reduces nanofluid velocity in the channel and tangential stresses on the channel walls, as seen in fig. 6. To overcome the resistance force of the porous medium the fluid *expends* a portion of its energy which is transformed into heat energy. This amount of heat is larger for all higher values of the porosity factor which leads to higher temperatures in the channel, as shown in fig. 7. As the porosity factor increases the exchanged amount of heat between the nanofluid and the bottom wall increases and the amount exchanged between the fluid and the top wall decreases. The bottom wall acts as a cooling radiator while the top wall is being cooled. These

conclusions are confirmed by the results given in tab. 2. A minus sign at the friction values on the upper wall indicates that the tangent to the velocity profile makes an obtuse angle with the O*x*-axis.

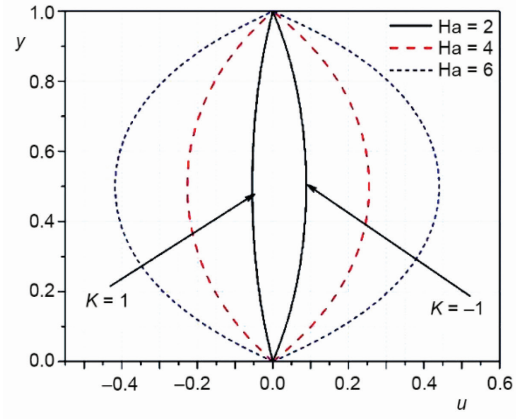

Figure 2. Velocity profiles for different Hartmann values

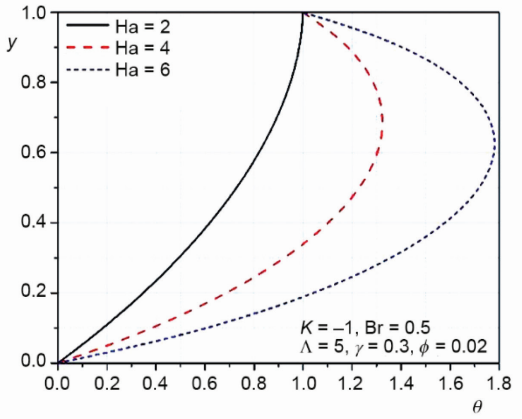

Figure 3. Temperature profiles for different Hartmann values

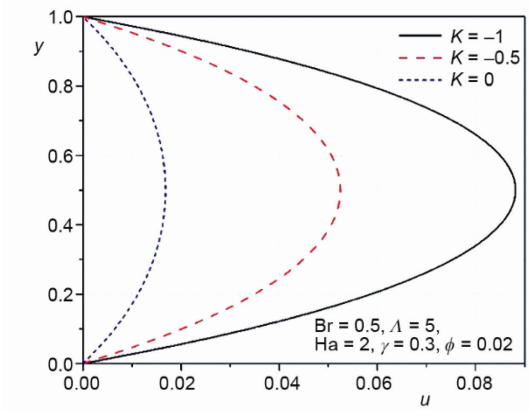

Figure 4. Velocity profiles for different *K* values

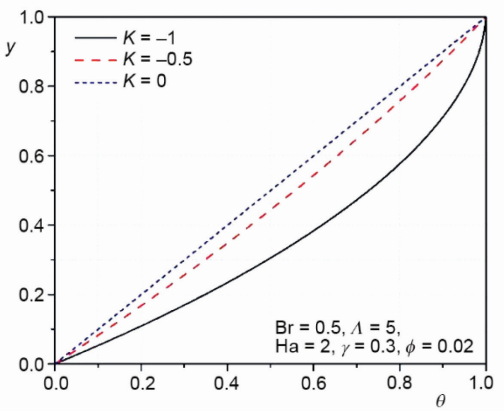

Figure 5. Temperature profiles for different *K* values

When the nanoparticle volume fraction increases, all the other factors remaining constant, the dynamic viscosity of the nanofluid also increases. Likewise as the dynamic viscosity increases so do the viscous force intensity and viscous dissipation. That is why higher nanoparticle volume fractions correspond to lower velocities and higher temperatures of the nanofluid in the channel, as shown in figs. 8 and 9, respectively. For higher volume fractions the exchanged amount of heat is larger between the nanofluid and the bottom wall and smaller between the nanofluid and the top wall.

Changes of the Casson factor also alter the viscous stress of the fluid. As the Casson factor increases the viscous stress decreases and so do the viscous force intensity and viscous dissipation. This in turn increases nanofluid velocity and decreases its temperature in the channel, as shown in figs. 10 and 11. Tangential stresses on the channel walls increase whereas the amount of exchanges heat between the nanofluid and the bottom wall decreases.

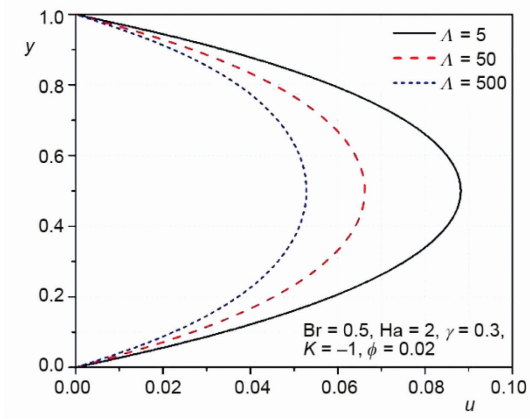

Figure 6. Velocity profiles for different Λ values

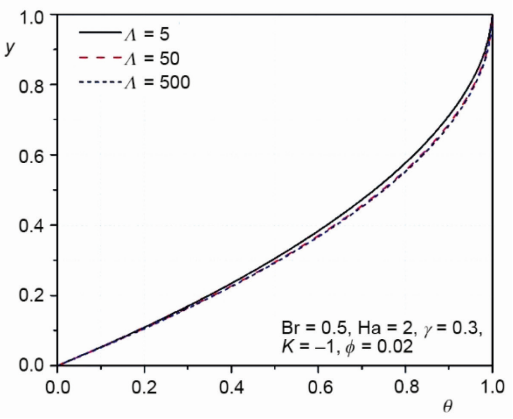

Figure 7. Temperature profiles for different Λ values

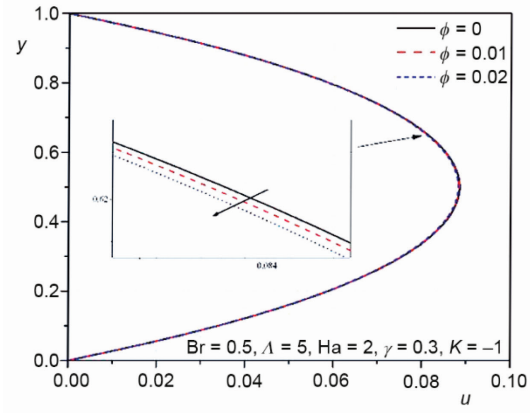

Figure 8. Velocity profiles for different ϕ values

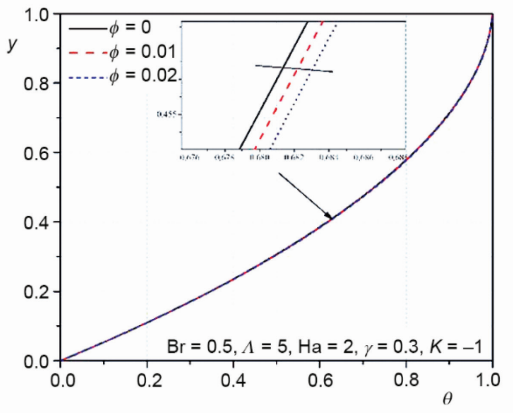

Figure 9. Temperature profiles for different ϕ values

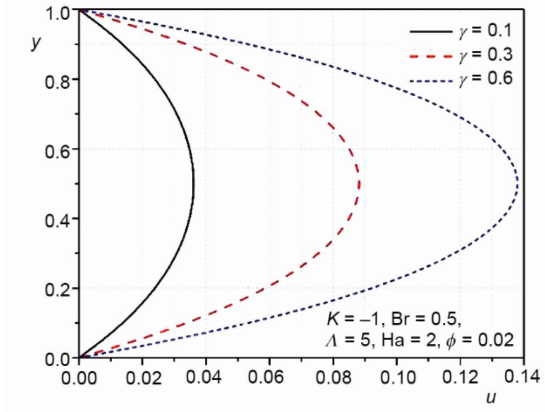

Figure 10. Velocity profiles for different γ values

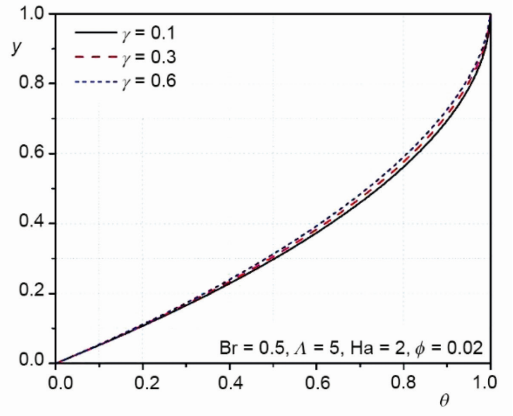

Figure 11. Temperature profiles for different γ values

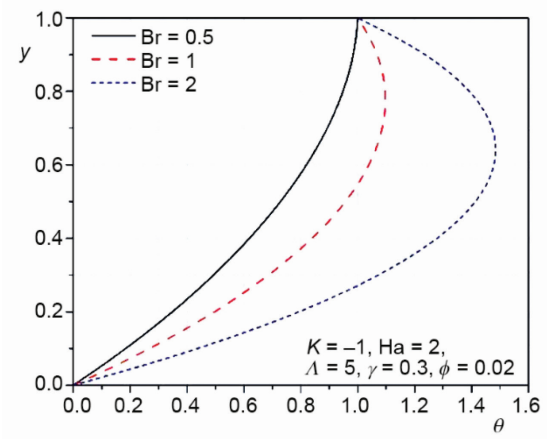

Figure 12. Temperature profiles for different Brinkman values

When the Brinkman number values change, all the other factors remaining constant, the temperature difference between the bottom and top wall also changes. The presented results correspond to cases when top wall temperatures are higher than bottom wall temperatures. Figure 12 shows that higher Brinkman values correspond to higher nanofluid temperatures in the channel and larger amounts of exchanged heat on the bottom and top wall. The bottom wall acts as a cooling radiator for each given Brinkman value but the top wall acts as a cooling radiator only for Br = 1 and Br = 2, while being cooled for Br = 0.5.

Result verification

To verify the obtained results the analyzed problem is reduced to the problem investigated in Petrović [30]. The selected values are $\phi = 0$ and $\gamma \to \infty$ which reduces the EMHD flow and heat transfer of the Casson nanofluid to EMHD flow and heat transfer of a Newtonian fluid. The following parameter values were used: Ha = 1, $\Lambda = 5$, Br = 1.4, and $K = -1$. The velocity and temperature distribution results obtained in the present study and those obtained in [30] are compared in figs. 13 and 14. The comparisons indicate that the overlap of the results is quite satisfactory.

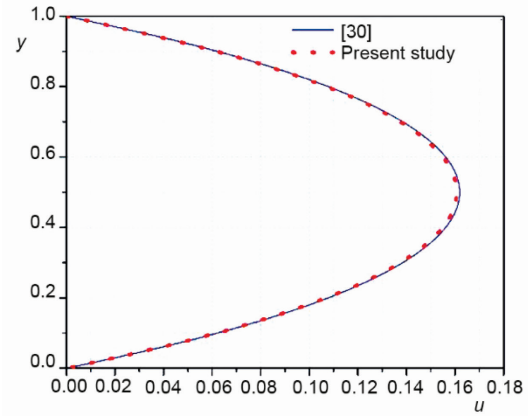

Figure 13. Comparison of velocity profiles

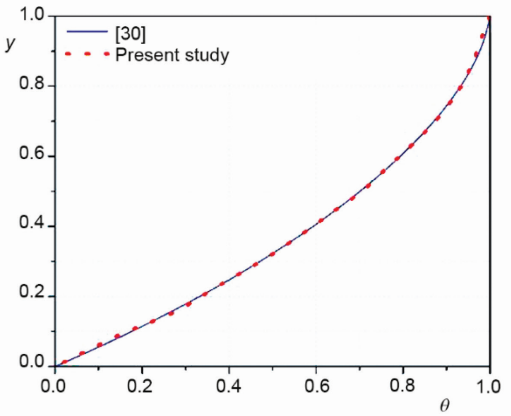

Figure 14. Comparison of temperature profiles

Conclusions

This paper investigated the EMHD flow and heat transfer of a Fe_3O_4-blod Casson nanofluid in a horizontal channel filled with a porous medium and with the bottom wall temperature exceeding the top wall temperature. The analysis of the obtained results yielded multiple conclusions.

Higher velocities and temperatures of the nanofluid in the channel correspond to higher absolute values of the external power factor and increased Hartmann number. Increase in the porosity factor, Brinkman number, and volume fraction increases the temperature of the nanofluid in the channel while higher values of volume fraction, Casson and porosity factor decreases the velocity. When the sign of the power factor changes the flow direction also changes. In each considered case the bottom wall acted as a cooling radiator.

This analysis is limited to Fe_3O_4 nanoparticles and blood as the base fluid. Interested researchers can extend the study to other nanofluids, moving walls, porous or stretching walls, *etc.* in order to obtain the desired results.

Acknowledgment

This research was financially supported by the Ministry of Science, Technological Development and Innovation of the Republic of Serbia (Contract No. 451-03-47/2023-01/200109).

Nomenclature

h – width of the region [m]
B – magnetic induction [T]
k – thermal conductivity [$WK^{-1}m^{-1}$]
P – non-dimensional pressure [–]
K – permeability [m^2]

Greek symbols

θ – dimensionless temperature [–]
μ – dynamic viscosity [Pa·s]
ρ – density [kgm^{-3}]
σ – electrical conductivity [Sm^{-1}]
Λ – porosity factor [–]
τ – skin friction [–]
ϕ – volume fraction of the solid nanoparticles [–]

References

[1] Choi, S. U. S., Enhancing Thermal Conductivity of Fluids with Nanoparticles, *Developments and Applications of Non – Newtonian Flows*, *FED-vol.231/MD-vol. 66*, (2021), pp. 99-105
[2] Umavathi, J. C., Sheremet, M. A., Mixed Convection Flow of an Electrically Conducting Fluid in a Vertical Channel Using Robin Boundary Conditions with Heat Source/Sink, *European Journal of Mechanics B/Fluids, 55* (2016), Jan., pp. 132-145
[3] Linga Raju, T., Electro-Magnetohydrodynamic Two Fluid Flow of Ionized Gases with Hall and Rotation Effects, *Int. J. of Applied Mechanics and Engineering, 26* (2021), 4, pp. 128-144
[4] Lima, J. A., *et al,* A simple Approach to Analyze the Fully Developed Two–Phase Magnetoconvection Type Flows in Inclined Parallel-Plate Channels, *Latin American Applied Research, 46* (2016), 3, pp. 93-98
[5] Petrović, J., *et al.,* Porous Medium Magnetohydrodynamic Flow and Heat Transfer of Two Immiscible Fluids, *Thermal Science, 20* (2016), Suppl. 5, S1405-S1417
[6] Krishna, G., *et al*., Numerical Investigation of Entropy Generation in Microporous Channel with Thermal Radiation and Buoyancy Force. *Indian Journal of Physics, 93* (2019), 11, pp. 1465-1476
[7] Kasaein, A., *et al.,* Nanofluid Flow and Heat Transfer in Porous Media: *A Review of the Latest Developments, International Journal of Heat and Mass Transfer, 107* (2017), Apr., pp. 778-791
[8] Sharma, M. K., Manjeet, Nanofluid Flow and Heat Convection in a Channel Filled with Porous Medium, *Journal of International Academy of Physical Science, 21* (2017), 2, pp. 167-188
[9] Khanafer, K., Vafai, K., Applications of Nanofluids in Porous Medium: A Critical Review, *Journal of Thermal Analysis and Calorimetry, 135* (2019), July, pp. 1479-1492
[10] Sheremet, M. A., Applications of Nanofluids, *Nanomaterials, 11* (2021), 7, 1716
[11] Raveendra, N., *et al.,* Mass Transfer and Radiative Heat Transfer Flow of MHD Casson Fluid with Temperature Gradient Dependent Heat Sink and Internal Mass Diffusion in a Vertical Channel with Stretching Porous Walls, *Chemical and Process Engineering Research, 47,* (2017), pp. 34-43

[12] Omokhuale, E., Jabaka, M. L., Magnetohydrodynamic Casson Fluid Flow over an Infinite Vertical Plate with Chemical Reaction and Heat Generation, *American Journal of Computational Mathematics, 9*, (2019), 3, pp. 187-200
[13] Gireesha, B. J., Sindhu, S., Entropy Generation Analysis of Casson Fluid Flow Through a Vertical Microchannel Under Combined Effect of Viscous Dissipation, Joule heating, Hall Effect and Thermal Radiation, *Multidiscipline Modeling in Materials and Structures, 16* (2020), 4, pp. 713-730
[14] Eldabe, N. T., *et al.,* Electromagnetic Steady Motion of Casson fluid wit Heat and Mass Transfer Through Porous Medium Past a Shrinking Surface, *Thermal Science, 25* (2021), 1A, pp. 257-265
[15] Khaled, A. R. A., Vafai, K., The Role of Porous Media in Modeling Flow and Heat Transfer in Biological Tissues, *International Journal of Heat and Mass Transfer, 46* (2003), 26, pp. 4989-5003
[16] Srinivas, S., *et al.,* Flow and Heat Transfer of Gold – Blood Nanofluid in a Porous Channel with Moving/Stationary Walls, *Journal of Mechanics, 33* (2017), 3, pp. 395-404
[17] Noreen, S., *et al.,* Blood Flow Analysis with Considering Effects in Vertical Channel, *Applied Nanoscience, 7* (2017), Apr., pp. 193-199
[18] Akhtar, S., *et al.*, Mechanic of Non-Newtonian Blood Flow in an Artery Having Multiple Stenosis and Electroosmotic Effects, *Science Progress, 104* (2021), 3, pp. 1-15
[19] Srinivas J., *et al*., Entropy Generation Analysis of Radiative Heat Transfer Effects on Channel Flow of Two Immiscible Couple Stress Fluids, *Journal of the Brazilian Society of Mechanical Sciences and Engineering, 39* (2017), 6, pp. 2191-2202
[20] Petrović, J., *et al.,* Nanofluid Flow and Heat Transfer Between Horizontal Plates in Porous Media, *Proceedings*, 5th International Conference Mechanical Engineering in XXI Century, University of Niš, Faculty of Mechanical Engineering in Niš, Serbia, 2020, pp. 97-102
[21] Chinyoka, T., Makinde, O. D., Computational Dynamics of Arterial Blood Flow in the Presence of Magnetic Field and Thermal Radiation Therapy, *Advances in Mathematical Physics, 2014* (2014), Apr., 915640
[22] Das, S. *et al.*, Hall and ion Slip Currents Impact on Electromagnetic Blood Flow Conveying Hybrid Nanoparticles Through an Endoscope with Peristaltic Waves, *Bio Nano Science, 11* (2021), 3, pp. 770-792
[23] Khan, U., *et al.,* Numerical Simulation of a Non-Linear Coupled Differential System Describing a Convective Flow of Casson Gold-Blood Nanofluidthrough a Starched Rotating Rigid Disk in the Presence of Lorentz Forces and Non-linear Thermal Radiation, *Numerical Methods for Partial Differential Equations, 38* (2022), 3, pp. 308-328
[24] Sharma, B. K., *et al.,* Hemdynamical Analysis of MHD Two Phase Blood Flow Through a Curved Permeable Artery Having Variable Viscosity with Heat and Mass Transfer*, Biomechanics and Modeling in Mechanobiology, 21* (2022), 3, pp. 797-825
[25] Jawad, M., *et al.*, Analysys of Hybrid Nanofluid Stagnation Point Flow over Stretching Surface with Melting Heat Transfer, *Mathematical Problems in Engineering, 2022* (2022), 9469164
[26] Khan, Z., *et al.*, Magnetohydrodynamic Thin Film Flow through a Porous Stretching Sheet with the Impact of Thermal Radiation and Viscous Dissipation, *Mathematical Problems in Engineering, 2022* (2022), 1086847
[27] Rehman, A., *et al.,* Anayitical Analysis of Steady Flow of Nanofluid, Viscous Dissipation with Convective Boundary Condition, *Thermal Science, 26* (2022), Spec. Issue 1, pp. 405-410
[28] Rehman, A., *et al.,* Analytical Study of MHD Couple Stress Casson Nanofluid Flow Over Stretching Surface, *Thermal Science, 26* (2022), Spec. Issue 1, pp. 397-403
[29] Alharbi, F. M., *et al*., Bioconvection Due to Gyrotactic Microorganisms in Couple Stress Hybrid Nanofluid Laminar Mixed Convection Incompessible Flow with Magnetic Nanoparticles and Chemical Reaction as Carrier for Tageted Drug Delivery through Porous Streaching Sheet, *Molecules 26* (2021), 13, 3954
[30] Petrović, J., Magnetohydrodynamic Flow and Heat Transfer in Porous Media, Ph. D. thesis, University of Niš, Faculty of Mechanical Engineering in Niš, Serbia, 2019

Paper submitted: May 16, 2023
Paper revised: June 18, 2023
Paper accepted: June 27, 2023